energies

MDPI

Article

Optimal Scheduling Strategy for Urban Distribution Grid Resilience Enhancement Considering Renewable-to-Ammonia Coordination

Li Jiang [1], Fei Hu [1], Shaolei Zong [1], Hui Yan [1], Wei Kong [1], Xiaoguang Chai [1] and Lu Zhang [2,*]

[1] State Grid Wuxi Power Supply Company, Wuxi 214000, China; jiangl.wx@js.sgcc.com.cn (L.J.); hufei@js.sgcc.com.cn (F.H.); shlzong@js.sgcc.com.cn (S.Z.); yanh@js.sgcc.com.cn (H.Y.); kongw@js.sgcc.com.cn (W.K.); chaixg@js.sgcc.com.cn (X.C.)

[2] College of Information and Electrical Engineering, China Agricultural University, Beijing 100091, China

* Correspondence: zhanglu1@cau.edu.cn

Abstract: The integration of numerous distributed energy sources into the power system offers exciting opportunities to enhance the resilience of distribution networks. It is worth noting that the renewable-to-ammonia system has the potential to alleviate the multi-temporal and spatial imbalance of the power system. Therefore, this paper proposes a mathematical model for a renewable-to-ammonia system, taking into account the material balance and power balance of each unit. Based on this, this paper further explores the optimization scheduling method for flexible ammonia loads in distribution networks. A relaxation method for branch flow models in distribution networks based on second-order cone programming is proposed. An optimization scheduling model for flexible ammonia loads in distribution networks is constructed to minimize network loss. Moreover, considering the environmental advantages of the renewable-to-ammonia system, this paper compares the changes in hydrogen production technologies under different carbon emission constraints. Finally, a case study of the IEEE 33-node system is adopted to verify the effectiveness of the proposed model and method. It indicates that the renewable-to-ammonia system has environmental benefits and can reduce network loss to a certain extent.

Keywords: carbon emission; optimization scheduling; renewable-to-ammonia system; resilience enhancement; urban distribution network

Citation: Jiang, L.; Hu, F.; Zong, S.; Yan, H.; Kong, W.; Chai, X.; Zhang, L. Optimal Scheduling Strategy for Urban Distribution Grid Resilience Enhancement Considering Renewable-to-Ammonia Coordination. *Energies* **2024**, *17*, 4540. https://doi.org/10.3390/en17184540

Academic Editor: Wen-Hsien Tsai

Received: 27 July 2024
Revised: 22 August 2024
Accepted: 27 August 2024
Published: 10 September 2024

1. Introduction

In recent years, with the accelerated development of renewable energy in China, the inherent spatiotemporal imbalance between energy resources and demands has led to increasingly severe challenges with regard to consumption [1–3]. For example, there is a significant mismatch between the distribution of energy resources and energy consumption in China, which is particularly evident in the disparity between wind and solar resources in the Western and Three-North regions and the energy demand in these areas. Specifically, these regions are endowed with abundant renewable energy resources, such as wind and solar power, that are capable of generating substantial amounts of clean electricity. However, due to their relatively low levels of economic development, weak industrial infrastructure, and low population density and energy consumption levels, the demand for electricity in these regions is not high. This lack of demand leads to the underutilization of energy resources, preventing the full potential of renewable energy production from being realized. In addition, its uncertainty also poses threats to the safe and stable operation of the power system [4,5]. Therefore, it is necessary to explore new, adjustable resources on the demand side. Among many adjustment methods, producing hydrogen by water electrolysis has been widely regarded as an efficient means to mitigate renewable energy fluctuation, alleviate the multi-temporal and spatial imbalance of the power system, and achieve more extensive optimization of flexible resources [6–8].

Unlike electricity, hydrogen is also a raw material in the transportation, chemical, and construction industries. A series of processes, such as hydrogen storage, transmission, and consumption, still need to be considered after production. Therefore, it is essential to first consider the downstream utilization of hydrogen and then explore the flexibility of water electrolysis in the power system [9–11]. It is worth noting that ammonia production, as the largest hydrogen consumption area in China, has a concentrated demand for hydrogen and significant economies of scale, possessing the potential for large-scale consumption of renewable energy. Therefore, these distributed energy resources, such as renewable-to-ammonia systems, provide exciting opportunities to enhance the resilience of urban distribution networks [12,13].

Much work so far has focused on urban distribution network scheduling methods that include flexibility. The flexible resources that can be scheduled are mainly distributed across four aspects: source, network, load, and storage. On the node side, there are various distributed power supplies [14], nodes connected to the upper main network, a variety of controllable load [15–17] and energy storage devices [18], and an intelligent soft switch (SOP) on the grid side [19].

From the point of view of the node side, the day-ahead scheduling model of the urban distribution network is constructed to promote the consumption of renewable energy, which effectively reduces the amount of wind and light abandonment and network loss [20]. By integrating the distributed multi-energy storage system into the urban distribution network, the voltage regulation capacity of the urban distribution network is enhanced by the interaction of multi-energy loads. The results show that the proposed strategy can effectively alleviate the expected voltage overlimit problem [21]. A two-stage urban distribution network management method is proposed. The upper layer uses a dynamic optimal power flow model to reduce network loss, and the lower layer optimizes the power injection of the energy storage system to eliminate the imbalance at the common coupling points in the urban distribution network [22]. Considering multiple types of resources on the distribution side, including shared electric vehicle charging stations, distributed photovoltaic power supplies, and energy storage systems, an urban distribution network expansion planning model is proposed [23]. A temperature control characteristic model of air conditioning load is constructed, and a method of reducing pressure and regulating the temperature of the air conditioning load based on a multi-agent system is proposed [24]. In this paper, a load forecasting method for large-scale electric vehicle charging is proposed, and the influence of disordered charging on the network loss and voltage of the urban distribution network is analyzed [25]. In addition, the existing literature has studied the optimal scheduling strategies of various flexible load access urban distribution networks, such as electrolytic hydrogen production [26] and smart buildings [27].

From the point of view of the grid, aiming at the lowest possible transmission loss and reliability cost of the system network, the access scheme of SOP in an AC-DC hybrid distribution system is optimized and determined. The results show that the proposed method can effectively improve the reliability and economy of the system's operation [28]. Considering SOP, building heat storage, distributed power supply, and other resources, the steady-state SOP model is established, and its access scheme is planned. The example shows that SOP plays a complementary and coordinated role in the thermoelectric system [29]. Aiming at the annual comprehensive cost of the urban distribution network, the planning model of SOP is established to maximize the investment benefit [30]. By combining the energy storage system with SOP, the urban distribution network's robust optimization models of day-ahead hour level, day–day minute level, and real-time level are constructed to improve the voltage stability of the system [31]. A two-layer cooperative optimization method for the urban distribution network and SOP based on reinforcement learning is proposed, in which topological structure is dynamically selected at the upper layer and topological selection is modified at the lower layer, which effectively improves the flexibility of the urban distribution network operation and enables it to adapt to the uncertain scenario of the source load [32–34].

However, the above literature rarely considers the optimal scheduling methods of hydrogen downstream load access in the urban distribution network, ignoring its potential downstream adjustable ability [35–37]. Therefore, this paper pays further attention to the flexible operation mode of a renewable-to-ammonia system, which is beneficial for achieving a "grid-friendly" chemical industry cluster. The major contributions of this paper are as follows: First of all, we propose a mathematical model for a renewable-to-ammonia system, taking into account the material balance and power balance of the hydrogen production, storage, and utilization process. Secondly, based on the mathematical model and second-order cone programming, we propose an optimal dispatching model for the urban distribution network, considering the flexibility of the green ammonia industry with the lowest possible network loss as the objective function. Lastly, considering the environmental advantages of the renewable-to-ammonia system, this paper compares the changes in hydrogen production routes under low-hydrocarbon and clean-hydrogen constraints.

2. Process Design and System Modeling of Ammonia Production from Renewable Energy

This section mainly introduces the process flow and system modeling of the renewable-to-ammonia (RE2A) process. The RE2A system is shown in Figure 1.

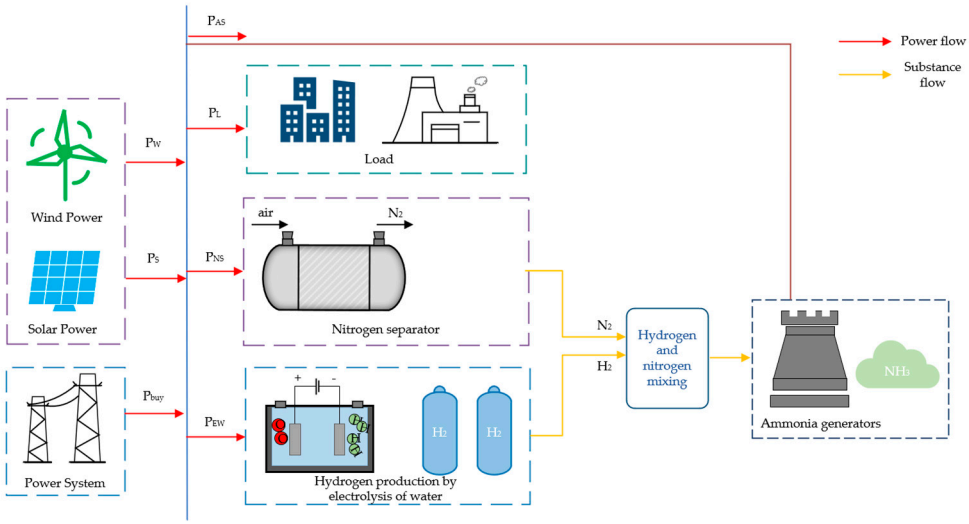

Figure 1. The schematic diagram of the renewable-to-ammonia system.

2.1. Renewable-to-Ammonia Technological Process

The RE2A process mainly consists of an air separation unit, a renewable energy electrolytic hydrogen production system, a hydrogen storage tank, and a synthetic ammonia unit. By harnessing wind and solar energy, water undergoes electrolysis to produce H_2 and O_2, as shown in Equation (1). As a stable gas flow rate is crucial for the synthesis of ammonia, the generated H_2 is directed into the hydrogen storage tank to adjust the gas flow rate within an appropriate range. Subsequently, the H_2 from the storage tank is proportionally mixed with N_2 obtained from the air separation unit, and then the hydrogen-to-nitrogen ratio of the synthesis gas is adjusted to 3:1 through nitrogen addition units. The compressed synthesis gas is introduced into the ammonia synthesis tower, where NH_3 is produced via the H-B process at temperatures of 350–550 °C and pressures of 10–46 MPa, as depicted in Equation (2). Finally, liquid ammonia is separated from the gas mixture during the cooling stage.

$$H_2O \rightarrow H_2 + \frac{1}{2}O_2, \Delta H^{o}_{298K} = 285.8 kJ/mol \quad (1)$$

$$N_2 + H_2 \rightleftharpoons 2NH_3, \Delta H^{o}_{298K} = -92.4 kJ/mol \quad (2)$$

Compared with the traditional coal ammonia production process, the renewable energy green ammonia production process has differences in raw gas production, power sources, and other aspects. For example, the air separation and compression cooling in the renewable energy green ammonia production process uses electric energy instead of coal to provide power. Apart from the above differences, the process flow of the two is basically the same, and the green ammonia production process from renewable energy is also known as the "green H-B process".

2.2. Renewable-to-Ammonia System Model

2.2.1. Constraint on Material Flow Balance

According to Equation (2) mentioned earlier, the ratio of hydrogen, nitrogen, and ammonia in the ammonia synthesis reactor is 3:1:2.

$$\mathrm{m}_t^{\mathrm{H_2,out}} : \mathrm{m}_t^{\mathrm{N_2}} : \mathrm{m}_t^{\mathrm{NH_3}} = 3 : 1 : 2, \forall t \in \mathrm{T}, \tag{3}$$

where $m_t^{\mathrm{H_2,out}}$ is the rate of H_2 consumption in the RE2A process; $m_t^{\mathrm{N_2}}$ is the rate of N_2 consumption in the RE2A process; and $m_t^{\mathrm{NH_3}}$ is the rate of NH_3 production in the RE2A process.

2.2.2. Power Balance Constraint

Based on the renewable energy-based ammonia production process, the power generation side primarily includes solar power, wind power, and power systems. On the consumption side, the main components are hydrogen electrolysis, air separation for nitrogen, user loads, and ammonia synthesis. Among these, ammonia synthesis, hydrogen electrolysis, and air separation for nitrogen are flexible loads that can participate in the power balance adjustment on the distribution network side. The formula for this process is as follows:

$$P_t^{\mathrm{WP}} + P_t^{\mathrm{PV}} + P_t^{\mathrm{RE2A,grid}} = P_t^{\mathrm{EW}} + P_t^{\mathrm{NS}} + P_t^{\mathrm{AS}}, \forall t \in \mathrm{T}, \tag{4}$$

$$P_t^{\mathrm{NS}} = \phi m_t^{\mathrm{N_2}} = \frac{1}{3}\phi m_t^{\mathrm{H_2,out}}, \forall t \in \mathrm{T}, \tag{5}$$

$$P_t^{\mathrm{AS}} = \psi m_t^{\mathrm{NH_3}} = \frac{2}{3}\psi m_t^{\mathrm{H_2,out}}, \forall t \in \mathrm{T}, \tag{6}$$

where P_t^{WP} is the generation of wind power; P_t^{PV} is the generation of photovoltaic power; P_t^{EW} is the power consumption of hydrogen production in the RE2A process; P_t^{NS} is the power consumption of air separation in RE2A process; P_t^{AS} is the power consumption of ammonia synthesis in RE2A process; $P_t^{\mathrm{RE2A,grid}}$ is the purchased electricity quantity for the RE2A process; ϕ is the energy consumption coefficient of air separation in the RE2A process; and ψ is the energy consumption coefficient of ammonia synthesis in the C2A process.

Constraint (4) represents the limit for the power balance at each moment. Constraints (5) and (6) represent the power consumption of nitrogen separation and ammonia synthesis, respectively.

2.2.3. Constraints of the Electrolytic Cells

$$C_{t+1}^{\mathrm{HS}} = m_t^{\mathrm{H_2,in}} = \frac{\eta^{\mathrm{EW}} P_t^{\mathrm{EW}} \cdot 3600}{\mathrm{HHV}}, \forall t \in \mathrm{T}, \tag{7}$$

$$\mu_t^{\mathrm{EW}} k^{\mathrm{EW,min}} C^{\mathrm{EW}} \le P_t^{\mathrm{EW}} \le \mu_t^{\mathrm{EW}} k^{\mathrm{EW,max}} C^{\mathrm{EW}}, \forall t \in \mathrm{T}, \tag{8}$$

where $m_t^{\mathrm{H_2,in}}$ is the rate of electrolytic hydrogen production or the rate of hydrogen flowing into the hydrogen storage tank; η^{EW} is the efficiency of electrolytic hydrogen production; HHV is the high calorific value of hydrogen; μ_t^{EW} is the start–stop variable of the electrolytic cell; $k^{\mathrm{EW,max}}$ is the upper limit of the electrolytic cell load; and $k^{\mathrm{EW,min}}$ is the lower limit of the electrolytic cell load.

2.2.4. Constraints of the Energy Storage Unit

$$C_{t+1}^{\mathrm{HS}} = C_t^{\mathrm{HS}} + \left(\eta^{\mathrm{HS}} m_t^{\mathrm{H_2,in}} - m_t^{\mathrm{H_2,out}} / \eta^{\mathrm{HS}}\right), \forall t \in \mathrm{T}, \tag{9}$$

$$C_0^{\mathrm{HS}} = C_T^{\mathrm{HS}}, \tag{10}$$

$$0 \le C_t^{\mathrm{HS}} \le C^{\mathrm{HS}}, \forall t \in \mathrm{T}, \tag{11}$$

where C_0^{HS} is the hydrogen storage capacity of the hydrogen storage tank at the initial time; C_t^{HS} is the hydrogen storage capacity of the hydrogen storage tank at time t; C_T^{HS} is the hydrogen storage capacity of the hydrogen storage tank at the final moment; and η^{HS} is the inflow and outflow efficiency of hydrogen in the hydrogen storage tank.

2.2.5. Constraints of Ammonia Synthesis Unit

$$\mu_t^{\mathrm{AS}} k^{\mathrm{AS,min}} m_t^{\mathrm{NH_3}} \le m_t^{\mathrm{H_2,out}} \le \mu_t^{\mathrm{AS}} k^{\mathrm{AS,max}} m_t^{\mathrm{NH_3}}, \forall t \in \mathrm{T}, \tag{12}$$

$$-r^{\mathrm{down}} m_t^{\mathrm{NH_3}} \le m_{t+1}^{\mathrm{H_2,out}} - m_t^{\mathrm{H_2,out}} \le r^{\mathrm{up}} m_t^{\mathrm{NH_3}}, \forall t \in \mathrm{T}, \tag{13}$$

where μ_t^{AS} is the start–stop variable of the synthetic ammonia reactor in the RE2A process; r^{down} is the landslide rate of hydrogen flowing into the ammonia reactor; and r^{up} is the climb rate of hydrogen flowing into the ammonia synthesis reactor.

Constraint (12) represents the lower and upper limits of the hydrogen outflow rate. Constraint (13) represents the ramp-up and ramp-down limits for ammonia synthesis reactors.

2.2.6. Renewable Energy Output Constraints

$$0 \le P_t^{\mathrm{WP}} \le \sum P_{t,\mathrm{max}}^{\mathrm{WP}}, \forall t \in \mathrm{T}, \tag{14}$$

$$0 \le P_t^{\mathrm{PV}} \le \sum P_{t,\mathrm{max}}^{\mathrm{PV}}, \forall t \in \mathrm{T}, \tag{15}$$

where $P_{s,t,max}^{\mathrm{WP}}$ is the maximum amount of electricity generated by wind power; $P_{s,t,max}^{\mathrm{PV}}$ is the maximum amount of electricity generated by photovoltaics.

3. Distribution Network Scheduling Model

3.1. Objective Function

Electrolytic hydrogen production and synthetic ammonia can be used as flexible resources that can be dispatched in the distribution network to promote the consumption of renewable energy and adjust the power balance. This section considers the minimum network transmission loss as the objective function to optimize the operation mode of the distribution network. The objective function can be expressed as follows:

$$\min \sum_{t \in \mathrm{T}} P_t^{\mathrm{Loss}} \tag{16}$$

$$P_t^{\mathrm{Loss}} = \sum_{ij \in E} I_{ij,t}^2 r_{ij}, \forall t \in \mathrm{T} \tag{17}$$

where P_t^{Loss} is the sum of the active losses; I_{ij} is the tributary current; r_{ij} is the branch resistance.

3.2. Operational Constraints

The operational constraints include renewable-to-ammonia system constraints, branch power flow constraints of distribution networks, power balance constraints, and carbon emission constraints, which are introduced in sequence below.

3.2.1. Renewable-to-Ammonia System Constraints

Constraints related to ammonia production from renewable energy sources have been elaborated on in the previous chapters. They mainly include the material flow balance constraint Formula (3), the electrolytic cell constraint Formulas (7) and (8), the power consumption constraint Formulas (5) and (6), the hydrogen storage tank constraint Formulas (9)–(11), the renewable energy output constraint Formulas (14) and (15), the ammonia production upper and lower limit constraint Formula (12), and the synthetic ammonia climbing constraint Formula (13).

3.2.2. Distribution Network Branch Power Flow Constraints

The power flow model for distribution network branches can be described as follows:

$$P_{j,t}^{\text{in}} = \sum_{l \in \delta(j)} P_{jl,t} - \sum_{i \in \pi(j)} \left(P_{ij,t} - I_{ij,t}^2 r_{ij} \right), \ \forall j \in \text{B} \tag{18}$$

$$Q_{j,t}^{\text{in}} = \sum_{l \in \delta(j)} Q_{jl,t} - \sum_{i \in \pi(j)} \left(Q_{ij,t} - I_{ij,t}^2 x_{ij} \right), \ \forall j \in \text{B}, \tag{19}$$

$$V_{j,t}^2 = V_{i,t}^2 - 2\left(P_{ij,t} r_{ij} + Q_{ij,t} x_{ij}\right) + I_{ij,t}^2 \left(r_{ij}^2 + x_{ij}^2 \right), \ \forall ij \in \text{E} \tag{20}$$

$$I_{ij,t}^2 = \frac{P_{ij,t}^2 + Q_{ij,t}^2}{V_{i,t}^2}, \ \forall ij \in \text{E}, \tag{21}$$

$$\underline{I}_{ij} \le I_{ij,t} \le \overline{I}_{ij}, \ \forall ij \in \text{E} \tag{22}$$

$$\underline{V}_j \le V_{j,t} \le \overline{V}_j, \forall j \in \text{B} \tag{23}$$

where $P_{j,t}^{\text{in}}$ is node j, which injects active power; $P_{ij,t}$, $P_{jl,t}$ is the active power at the head of the branch ij, jl; $Q_{j,t}^{\text{in}}$ is node j, which injects active power; $Q_{ij,t}$, $Q_{jl,t}$ is the reactive power at the head end of branch ij, jl; x_{ij} is branch reactance; $\underline{I}_{ij}$ is the lower branch current limit; $\overline{I}_{ij}$ is the upper limit of the branch current; $V_{i,t}$, $V_{j,t}$ is the node voltage; $\underline{V}_j$ is the node voltage lower limit; $\overline{V}_j$ is the node voltage cap; B is a collection of all nodes; E is a collection of all the slip roads; $\delta(j)$ is a set of branch end nodes with j as the first node; and $\pi(j)$ is a collection of nodes at the head of a branch with j as the end node.

The above constraints can be divided into equality constraints and inequality constraints, wherein the equality constraints are the active power balance constraint (18), the reactive power balance constraint (19), the voltage and current relationship constraint (20), and the power and voltage and current relationship constraint (21). The inequality constraints are the branch current safety constraint Formula (22) and the node voltage safety constraint Formula (23).

It should be noted that BFM type (21) is a quadratic constraint, resulting in a nonlinear programming model. Here, let $\widetilde{I}_{ij,t} = I_{ij,t}^2$ and $\widetilde{V}_{ij,t} = V_{ij,t}^2$ and relax the equality constraint to an inequality constraint, which can be written as follows:

$$P_{ij,t}^2 + Q_{ij,t}^2 \le \widetilde{I}_{ij,t} \widetilde{V}_{j,t}, \ \forall ij \in \text{E} \tag{24}$$

Second-order conic relaxation (SOCR) is performed on Equation (24) by introducing the second-order conic constraint.

$$\left\| \begin{matrix} 2P_{ij,t} \\ 2Q_{ij,t} \\ \widetilde{I}_{ij,t} - \widetilde{V}_{j,t} \end{matrix} \right\|_2 \le \widetilde{I}_{ij,t} + \widetilde{V}_{j,t}, \ \forall ij \in \text{E} \tag{25}$$

The optimal power flow problem has completed its transformation from a nonlinear programming problem to a convex optimization problem, and the difficulty of solving it has significantly decreased.

3.2.3. Power Balance Constraints

The power balance constraints can be described as follows:

$$P_{i,t}^{\mathrm{in}} = P_{i,t}^{\mathrm{WP}} + P_{i,t}^{\mathrm{PV}} - P_{i,t}^{\mathrm{EW}} - P_{i,t}^{\mathrm{NS}} - P_{i,t}^{\mathrm{AS}} - P_{i,t}^{\mathrm{L}}, \forall i \in \mathrm{B}, t \in \mathrm{T} \tag{26}$$

$$Q_{i,t}^{\mathrm{in}} = -Q_{i,t}^{\mathrm{L}}, \forall i \in \mathrm{B}, t \in \mathrm{T} \tag{27}$$

where $P_{i,t}^{L}$ is the active power required for the load at node i; $Q_{i,t}^{L}$ is the reactive power required for the load at node i.

3.2.4. Carbon Emission Constraints

Compared with the traditional coal ammonia production process, the advantage of renewable energy ammonia production is that it is clean with no carbon emission, and that it has good environmental benefits. Therefore, the carbon emission constraint of hydrogen production is set here, and the change in hydrogen production methods from ammonia from coal to ammonia from renewable energy sources is compared under the constraints of the no-carbon-emission constraint, the low-hydrocarbon constraint, and the clean hydrogen and renewable hydrogen constraint.

$$f^{\mathrm{coal}} \sum_{i \in \mathrm{B}} \sum_{t \in \mathrm{T}} \dot{n}_{i,t}^{\mathrm{H_2}} \leq \mathrm{M} \sum_{i \in \mathrm{B}} \sum_{t \in \mathrm{T}} (\dot{n}_{i,t}^{\mathrm{H_2}} + \dot{n}_{i,t}^{\mathrm{H_2,out}}), \tag{28}$$

where f^{coal} is the carbon emission coefficient of coal-to-hydrogen production, 25 $\mathrm{kgCO_2/kgH_2}$; M is the carbon emission threshold for hydrogen production.

According to the green hydrogen certification standard issued by the China Hydrogen Energy Alliance, when considering the low-carbon hydrogen constraint, the value of M is 14.51 $\mathrm{kgCO_2/kgH_2}$. When considering the constraints of clean hydrogen and renewable hydrogen, the value of M is 4.9 $\mathrm{kgCO_2/kgH_2}$.

4. Case Study

4.1. Data Description

In this example, the IEEE33-node system is used to further verify the optimal scheduling method of the distribution network with a flexible load of ammonia production from renewable energy sources. In the IEEE33-node system, two renewable energy ammonia plants, RE2A1 and RE2A2, are connected at nodes 33 and 18, respectively, where renewable power is provided by wind power plants and photovoltaic power plants. The thermal power plant is connected to node 19, and the photovoltaic power plant is connected to node 25. In addition, a coal-to-ammonia plant is connected at node 33 to compare the change in the hydrogen production technology path under the consideration of carbon emission constraints, as shown in Figure 2. In this example, the optimal scheduling period is 24 h, and the step is set to 1 h. It can be seen from the above that this problem is a mixed-integer second-order cone programming problem, which can be solved by CPLEX on the MATLAB-YALMIP R2020b platform.

In this example, three scenarios are set up to compare the impact of the renewable energy ammonia production system on the distribution network from different angles, as shown below:

1. Scenario 1: RE2A1 and RE2A2 provide renewable energy generation but are not used for ammonia production; C2A does not operate.
2. Scenario 2: RE2A1 and RE2A2 provide renewable energy generation and are used for ammonia production; C2A does not operate.

3. Scenario 3: RE2A1 provides renewable energy generation and is used for ammonia production; RE2A2 provides renewable energy generation but is not used for ammonia production; C2A operates ammonia production.

In the above scenario, scenario 1 and scenario 2 compare the influence of the synthetic ammonia flexible load on the safety state of the distribution network operation and show the optimal scheduling results for hydrogen ammonia. Scenario 3 compares the scheduling of RE2A and C2A in the distribution network under different carbon emission constraints for hydrogen production.

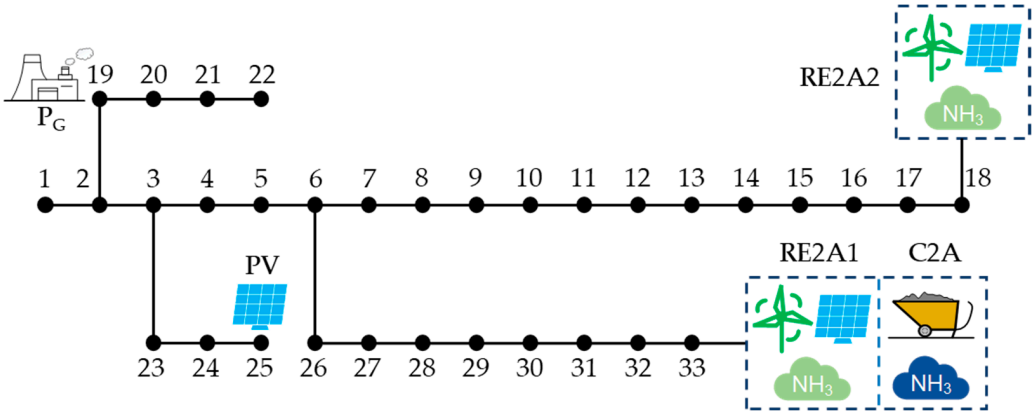

Figure 2. IEEE33 node system.

4.2. Optimizing Scheduling Results

This section mainly analyzes the results of the example based on three aspects: distribution network security, hydrogen and ammonia dispatching results, and environmental benefits.

4.2.1. Distribution Network Safety Analysis

This paper mainly reflects the safety state of lines and nodes from the network loss, power flow, and voltage distribution. Table 1 shows the network loss comparison between scenario 1 and scenario 2.

Table 1. Comparison of network losses in different scenarios.

	Scenario 1	**Scenario 2**
Network loss (kWh)	971.19	956.70

In scenario 1, wind power and photovoltaic power are not used for ammonia production, and the load at each node in the distribution network is constant. Therefore, the network loss of the distribution network in scenario 1 is relatively high. In scenario 2, the flexible load of electrolytic hydrogen production and synthetic ammonia can absorb part of the electricity when the wind or light resources are abundant, which can reduce the network loss to a certain extent.

In addition, this example analyzes the branch power flow distribution and node voltage distribution of the distribution network, considering the industrial flexibility of green ammonia, as shown in Figures 3 and 4.

As can be seen from the figures, there is no blocking of the lines in the distribution network within one day, and the voltage value of each node is 1 p.u. It fluctuates smoothly in the range of 1.05 p.u., and no voltage is too low or over the limit. Therefore, flexible and controllable load and power flow optimization can improve the stability of the distribution network operation.

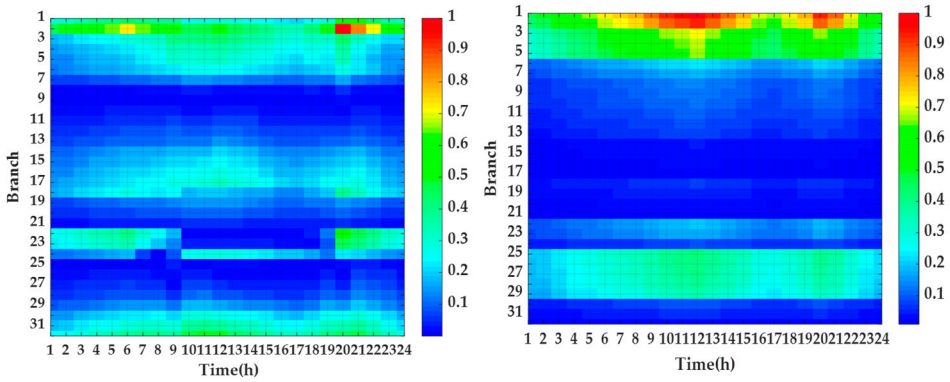

Figure 3. Twenty-four-hour node power flow distribution diagram.

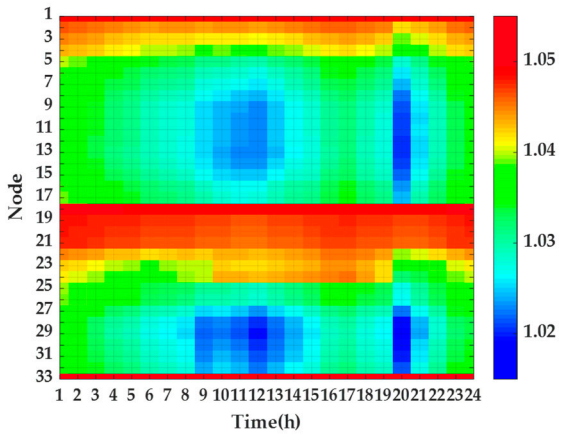

Figure 4. Twenty-four-hour node voltage distribution diagram.

4.2.2. Analysis of Hydrogen and Ammonia Dispatch Results

The production of hydrogen ammonia is shown in Figure 5. It can be found that from the perspective of total output, there is surplus renewable electricity for hydrogen production in the night gale period or in the noon sufficient light period, while in the evening peak period of electricity consumption, hydrogen production decreases significantly. The production of ammonia in the first few periods is relatively small, mainly due to the high power consumption of hydrogen production and the ability to produce ammonia after the completion of hydrogen production, while the production trends of ammonia and hydrogen in the latter period are similar.

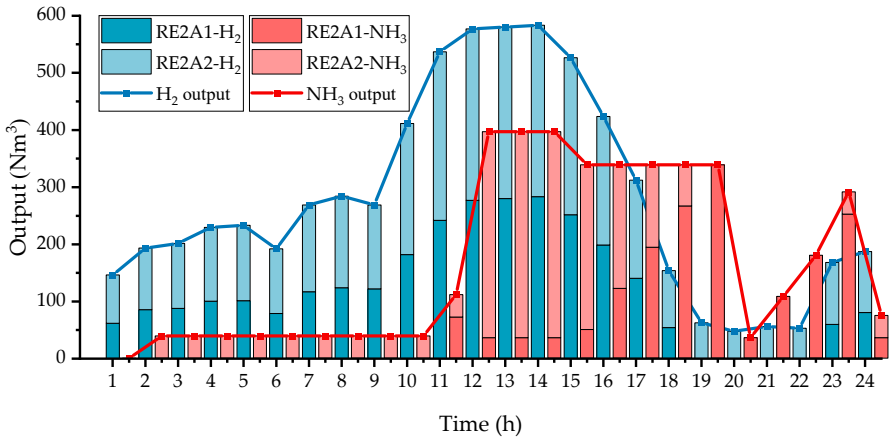

Figure 5. Hydrogen ammonia production.

From the perspective of RE2A systems connected at different nodes, the hydrogen production trends of RE2A1 and RE2A2 are similar. In contrast, the ammonia production of RE2A1 is mainly concentrated in the later period, while the ammonia production of RE2A2 is mainly concentrated in the earlier period. This is mainly because hydrogen production is closely related to the output trend of renewable energy, and there are hydrogen storage tanks in the process from the completion of hydrogen production to ammonia synthesis, and the optimal time period for ammonia production at different nodes can be determined according to the network loss of the line.

4.2.3. Environmental Benefit Analysis

Compared with the C2A system, the biggest advantage of the RE2A system is that it is clean and low-carbon. Figures 6 and 7, respectively, show the production of hydrogen under the low-hydrocarbon constraint and under the clean and renewable hydrogen constraint.

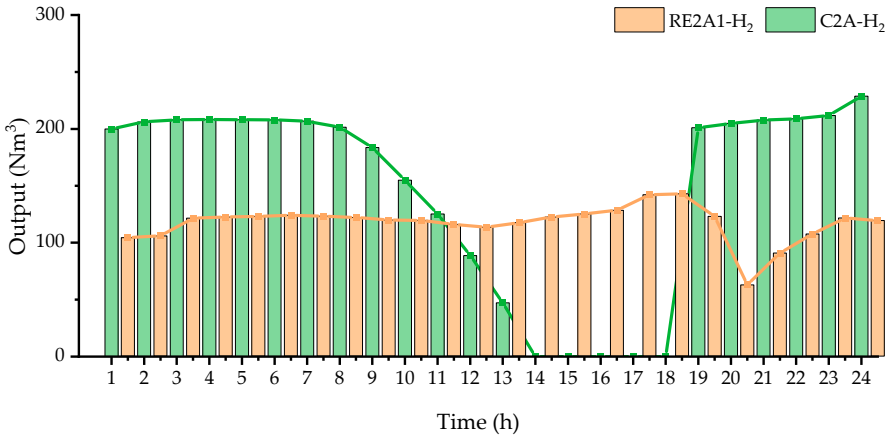

Figure 6. Hydrogen production under the constraints of low-carbon hydrogen.

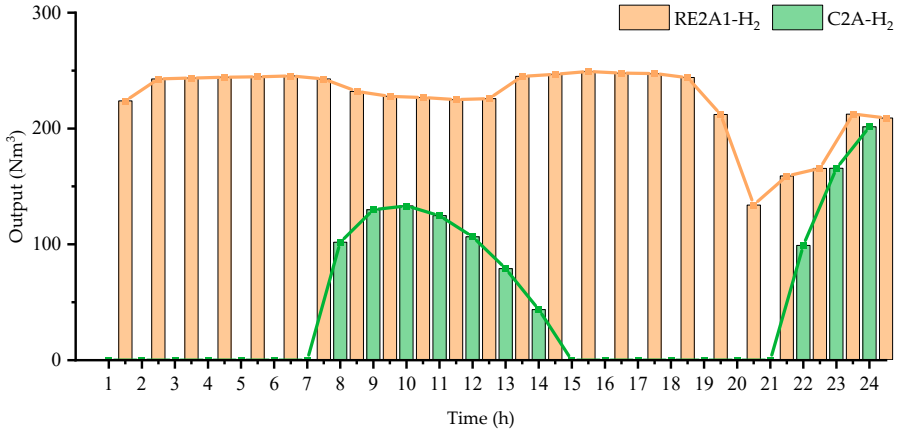

Figure 7. Hydrogen production under the constraints of clean hydrogen.

When there is no carbon emission constraint, all hydrogen is produced by C2A. The hydrogen production of RE2A and C2A is equivalent after considering the low-hydrocarbon constraint. After considering the constraints of clean hydrogen and renewable hydrogen, the hydrogen production of RE2A increased significantly. This indicates that in the context of the low-carbon energy transition, RE2A will have more significant advantages.

In summary, considering the optimal scheduling of the green ammonia industry flexibility in the distribution network can reduce network loss to a certain extent and ensures that the power flow and voltage in the distribution network are in a safe state. In addition, the technical route of ammonia production from renewable energy can promote the transformation of the chemical industry to a low-carbon energy economy.

The choice of ammonia production pathways primarily aims to highlight the significant environmental advantages of using renewable energy for ammonia synthesis compared to traditional coal-based methods. Utilizing renewable energy for ammonia synthesis can effectively reduce greenhouse gas emissions and lower environmental pollution, aligning with global sustainability goals and contributing to climate change mitigation. In contrast, traditional coal-based ammonia production consumes substantial amounts of fossil fuels and emits significant quantities of carbon dioxide and other harmful substances, placing a considerable burden on the environment.

In this context, the focus of this discussion is to showcase the environmental benefits of renewable energy-based ammonia production, emphasizing its positive role in reducing carbon footprints and promoting the development of green industry. Consequently, although economic factors such as production costs, investment requirements, and operational expenses are important considerations for practical implementation, this discussion does not delve into a detailed comparison of these costs. The primary objective is to underline the environmental advantages of renewable energy technologies, rather than to compare the economic costs of various production pathways.

This paper uses the IEEE33-node system for case study analysis primarily to demonstrate the feasibility of the renewable energy-based ammonia production system in reducing network losses and enhancing system security within the distribution network. The analysis indicates that the renewable energy ammonia production system has significant regulatory potential and can also be applied to other large-scale distribution network systems, such as IEEE141, due to their similar topological structures. The focus of this paper is to showcase the effectiveness of the proposed method in distribution networks, and therefore, validation of the case study was not performed across multiple systems.

5. Conclusions

In summary, the conclusions drawn from the paper are as follows: The renewable energy-based ammonia production system, as a new type of flexible resource on the demand side, can reduce network losses to some extent and can enhance the safety and resilience of urban power grids through the optimal scheduling of hydrogen and ammonia production. Additionally, compared to traditional coal-based ammonia production, the renewable energy ammonia production system offers significant environmental benefits.

This paper addresses the scheduling issues of green hydrogen chemical processes integrated into the power system, with ammonia as the final product, and provides optimization strategies for scheduling. Given the limited research on green hydrogen chemical systems in the power sector, future research could focus on the following aspects:

(1) This paper focuses on ammonia as a downstream product of hydrogen, and the findings are specific to this product. However, other chemical products, such as methanol, which have similar production processes to ammonia, could also be studied as downstream chemical products in further research.

(2) This paper only considers optimization scheduling strategies for green hydrogen chemical processes aimed at enhancing the safety of active distribution networks. As a flexible resource on the demand side, green hydrogen chemicals can provide ancillary services to the power system, such as peak shaving, frequency regulation, and reserves, due to their flexible control technologies. Exploring these market opportunities could enhance the market competitiveness of green hydrogen chemicals. Therefore, further research on the role of green hydrogen chemical systems in power balance regulation is needed.

(3) This paper considers hydrogen energy solely as an electrification carrier for the chemical industry. However, green hydrogen chemical systems involve multiple sectors, including power generation, hydrogen production, and chemical processes, with transactions across various markets such as electricity, hydrogen, carbon, and ammonia. Different sectors may be managed by different market investors. Therefore, a key focus for future research will be on exploring how to reasonably coordinate the distribution of benefits while ensuring overall efficiency.

Author Contributions: Conceptualization, L.J. and F.H.; methodology, S.Z.; software H.Y.; validation, W.K., X.C. and F.H.; formal analysis, L.J.; investigation, S.Z.; resources, H.Y.; data curation, L.J.; writing—original draft preparation, F.H.; writing—review and editing, S.Z.; visualization, W.K.; supervision, L.Z. and X.C.; project and administration, L.J.; funding acquisition, S.Z. All authors have read and agreed to the published version of the manuscript.

Funding: This research was funded by Research and Application of Resilience Enhancement Technology for Urban Power Grids in Response to Extreme Natural Disasters, grant number J2023170.

Data Availability Statement: The original contributions presented in the study are included in the article, further inquiries can be directed to the corresponding author.

Conflicts of Interest: The authors declare no conflicts of interest. Authors Li Jiang, Fei Hu, Shaolei Zong, Hui Yan, Wei Kong and Xiaoguang Chai were employed by the State Grid Wuxi Power Supply Company. The remaining author declares that the research was conducted in the absence of any commercial or financial relationships that could be construed as a potential conflict of interest.

References

1. Wu, Z.; Wang, J.; Zhong, H.; Gao, F.; Pu, T.; Tan, C.W.; Chen, X.; Li, G.; Zhao, H.; Zhou, M.; et al. Sharing economy in local energy markets. *J. Mod. Power Syst. Clean Energy* **2022**, *11*, 714–726. [CrossRef]
2. Wang, J.; Gao, F.; Zhou, Y.; Guo, Q.; Tan, C.W.; Song, J.; Wang, Y. Data sharing in energy systems. *Adv. Appl. Energy* **2023**, *10*, 100132. [CrossRef]
3. Guo, C.; Luo, F.; Yang, J.; Sun, M.; Cai, Z. Transactive Operational Framework for Internet Data Centers in Geo-Distributed Local Energy Markets. *IEEE Trans. Cloud Comput.* **2022**, *11*, 1133–1143. [CrossRef]
4. Yang, J.; Zhao, J.; Qiu, J.; Wen, F. A Distribution Market Clearing Mechanism for Renewable Generation Units with Zero Marginal Costs. *IEEE Trans Ind. Inform.* **2019**, *15*, 4775–4787. [CrossRef]
5. Akhter, Q.; Siddique, A.; Alqahtani, S.A.; Mahmood, A.; Alam, M.; Mushtaq, Z.; Qureshi, M.F.; Aslam, W.; Pathak, P.K. Efficient Energy Management for Household: Optimization-Based Integration of Distributed Energy Resources in Smart Grid. *IEEE Access* **2023**, *11*, 85716–85727. [CrossRef]
6. Yang, J.; Dong, D.; Wen, F.; Chen, G.; Qiao, Y. A Decentralized Distribution Market Mechanism Considering Renewable Generation Units with Zero Marginal Costs. *IEEE Trans. Smart Grid* **2020**, *11*, 1724–1736. [CrossRef]
7. Shang, J.; Wang, K.; Lai, X.; Yang, J.; Jiang, X.; Gao, J. Spot Electricity Market Design Considering Carbon Emissions for a Power System with a High Penetration of Renewable Energy Generation. *IEEE Trans Netw. Sci. Eng.* **2024**, *accepted for publication*.
8. Yu, Y.; Wang, J.; Chen, Q.; Urpelainen, J.; Ding, Q.; Liu, S.; Zhang, B. Decarbonization efforts hindered by China's slow progress on electricity market reforms. *Nat. Sustain.* **2023**, *6*, 1006–1015. [CrossRef]
9. Ma, J.; Kong, H.; Wang, J.; Zhong, H.; Li, B.; Song, J.; Kammen, D.M. Carbon-neutral pathway to mitigating transport-power grid cross-sector effects. *Innov.* **2024**, *5*, 100611. [CrossRef] [PubMed]
10. Wang, J.; Wu, Z.; Du, E.; Zhou, M.; Li, G.; Zhang, Y.; Yu, L. Constructing a V2G-enabled regional energy Internet for cost-efficient carbon trading. *J. Power Energy Syst.* **2020**, *6*, 31–40.
11. Zheng, L.; Wang, J.; Yu, Y.; Li, G.; Zhou, M.; Xia, Q.; Xu, G. On the consistency of renewable-to-hydrogen pricing. *J. Power Energy Syst.* **2022**, *8*, 392–402.
12. Wang, Z.; Gao, J.; Zhao, R.; Wang, J.; Li, G. Optimal bidding strategy for virtual power plants considering the feasible region of vehicle-to-grid. *IET Energy Convers. Econ.* **2020**, *1*, 1–13. [CrossRef]
13. Wang, J.; Zhong, H.; Qin, J.; Tang, W.; Rajagopal, R.; Xia, Q.; Kang, C. Incentive mechanism for sharing distributed energy resources. *J. Mod. Power Syst. Clean Energy* **2019**, *7*, 837–850. [CrossRef]
14. Zhao, Y.; Zhang, G.; Hu, W.; Huang, Q.; Chen, Z.; Blaabjerg, F. Meta-learning based voltage control for renewable energy integrated active distribution network against topology change. *IEEE Trans. Power Syst.* **2023**, *38*, 5937–5940. [CrossRef]
15. Su, L.; Li, Z.; Jin, X.; Xia, M.; Chen, Q. Distributed energy management strategy with active distribution network for smart buildings based on opportunity-constrained planning. *Proc. CSEE* **2023**, *43*, 3781–3794.
16. Yan, H.; Hu, J.; Huang, D.; Zhang, Z.; Yue, Y. Distribution network planning that considers EV virtual power plant flexibility and high proportion of PV access. *Power Constr.* **2022**, *43*, 14–23.
17. Li, Z.; Su, S.; Jin, X.; Chen, H. Distributed energy management for active distribution network considering aggregated office buildings. *Renew. Energy* **2021**, *180*, 1073–1087. [CrossRef]
18. Li, X.; Wang, L.; Yan, N.; Ma, R. Cooperative Dispatch of Distributed Energy Storage in Distribution Network with PV Generation Systems. *IEEE Trans. Appl. Supercond.* **2021**, *31*, 1–4. [CrossRef]
19. Min, L.; Lou, C.; Yang, J.; Yu, J. Multi-objective operation optimization of active distribution network considering commutation soft switching three-phase unbalance adjustment. *Power Syst. Autom.* **2023**, *47*, 56–65.
20. Chen, Y.; Chang, J. EMaaS: Cloud-Based Energy Management Service for Distributed Renewable Energy Integration. *IEEE Trans. Smart Grid* **2015**, *6*, 2816–2824. [CrossRef]

21. Yu, P.; Wan, C.; Song, Y.; Jiang, Y. Distributed control of multi-energy storage systems for voltage regulation in distribution networks: A back-and-forth communication framework. *IEEE Trans. Smart Grid* **2021**, *12*, 1964–1977. [CrossRef]
22. Kalantar-Neyestanaki, M.; Cherkaoui, R. Coordinating distributed energy resources and utility-scale battery energy storage system for power flexibility provision under uncertainty. *IEEE Trans. Sustain. Energy* **2021**, *12*, 1853–1863. [CrossRef]
23. Wang, S.; Zhao, Y.; Chen, C.; Fan, H.; Luo, F. Expansion planning of active distribution networks with multiple distributed energy resources and EV sharing system. *IEEE Trans. Smart Grid* **2020**, *11*, 602–611. [CrossRef]
24. Zhou, Q.; Ma, R.; Wang, T.; Lu, P.; Feng, C.; Wu, W. Multi-agent based active distribution network air conditioning load aggregation and its pressure reduction and temperature reduction method. *Proc. CSEE* **2022**, *42*, 6668–6681.
25. Gautam, A.; Tariq, M.; Pandey, J.; Verma, K.; Urooj, S. Hybrid Sources Powered Electric Vehicle Configuration and Integrated Optimal Power Management Strategy. *IEEE Access* **2022**, *10*, 121684–121711. [CrossRef]
26. Li, J.; Lin, J.; Song, Y.; Xing, X.; Fu, C. Operation optimization of power to hydrogen and heat (P2HH) in ADN coordinated with the district heating network. *IEEE Trans. Sustain. Energy* **2019**, *10*, 1672–1683. [CrossRef]
27. Li, Z.; Su, L.; Jin, X.; Chen, H.; Wei, C.; Zhao, Z. Energy management strategies for smart buildings to improve wind power acceptance capacity. *Power Grid Technol.* **2021**, *45*, 2288–2298.
28. Jiang, W.; Su, X.; He, J.; Yang, L.; Duan, X.; Ju, L. Planning-operation collaborative optimization method for flexible soft switch access in AC and DC distribution networks. *Power Syst. Autom.* **2023**, *47*, 33–43.
29. Zhang, T.; Wang, J.; Zhong, H.; Li, G.; Zhou, M.; Zhao, D. Soft open point planning in renewable-dominated distribution grids with building thermal storage. *CSEE J. Power Energy Syst.* **2023**, *9*, 244–253.
30. Zhao, J.; Chen, H.; Song, G.; Fan, X.; Li, P.; Wu, J. A planning method for smart soft switches in distribution networks considering reliability benefits. *Power Syst. Autom.* **2020**, *44*, 22–31.
31. Ru, Q.; Mi, X.; Song, Z.; Liu, J.; Lei, X. Robust optimization of hybrid time scale of active distribution network considering energy storage-intelligent soft switching. *China Power* **2022**, *55*, 129–139.
32. Dong, L.; Wu, Y.; Zhang, T.; Wang, X.; Hao, Y.; Guo, L. A two-layer optimization method for active distribution network with intelligent soft switch based on reinforcement learning. *Power Syst. Autom.* **2023**, *47*, 59–68.
33. Zhao, X.; Wang, J.; Zhang, T.; Cui, D.; Li, G.; Zhou, M. A novel short-term load forecasting approach based on kernel extreme learning machine: A provincial case in China. *IET Renew. Power Gener.* **2022**, *16*, 2658–2666. [CrossRef]
34. Yu, Y.; Chen, L.; Wang, J.; Zhao, Y.; Song, J. Implications of Power Industry Marketization for Sustainable Generation Portfolios in China. *J. Clean. Prod.* **2022**, *378*, 134541. [CrossRef]
35. Itiki, R.; Manjrekar, M.; Di Santo, S.G. Proposed Extension of the U.S.–Caribbean Super Grid to South America for Resilience during Hurricanes. *Energies* **2024**, *17*, 233. [CrossRef]
36. Santos-Ramos, J.E.; Saldarriaga-Zuluaga, S.D.; López-Lezama, J.M.; Muñoz-Galeano, N.; Villa-Acevedo, W.M. Microgrid Protection Coordination Considering Clustering and Metaheuristic Optimization. *Energies* **2024**, *17*, 210. [CrossRef]
37. Vega Penagos, C.A.; Diaz, J.L.; Rodriguez-Martinez, O.F.; Andrade, F.; Luna, A.C. Metrics and Strategies Used in Power Grid Resilience. *Energies* **2024**, *17*, 168. [CrossRef]